Turkish Computational and Theoretical Chemistry

Turkish Comp Theo Chem (TC&TC)

Volume(Issue): 4(1) – Year: 2020 – Pages: 24-31

e-ISSN: 2602-3237

https://doi.org/10.33435/tcandtc.674902

Received: 15.01.2020 ***Accepted***: 27.05.2020 *Research Article*

Electronics structure and optical properties of $Mg(BiO_2)_4$ and $Mg(Bi_{0.91}Ge_{0.083}O_2)_4$: A first principle approach

Md. Tawhidul ISLAM [a], Ajoy KUMER [b, 1], Debashis HOWLADER [a], Kamal Bikash CHAKMA [a], Unesco CHAKMA [a]

[a] Department Electrical and Electronics Engineering, European University of Bangladesh, Gabtoli, Dhaka-1216, Bangladesh

[b] Department of Chemistry, European University of Bangladesh, Gabtoli, Dhaka-1216, Bangladesh

Abstract: The new compounds, $Mg(BiO_2)_4$ was synthesized and structurally characterized semiconductor. Due to theoretical investigation for both of $Mg(BiO_2)_4$ and $Mg(Bi_{0.91}Ge_{0.083}O_2)_4$, computational tools were used. To calculated the electronic band structures, the total density of state, the partial density of state, and optical properties were used Generalized Gradient Approximation (GGA) based on the Perdew–Burke–Ernzerhoff (PBE0) using first principle method for $Mg(BiO_2)_4$. The band gap was recorded 0.545 eV which is supported for good semiconductor. The density of states was simulated for evaluating the nature of 3s, 3p for Mg, 6s 6p, 4d, and 2s, 2p for O atoms. Furthermore, the optical properties including absorption, reflection, refractive index, conductivity, dielectric function, and loss function were simulated which can account for the superior absorption of the visible light. The key point of this research to determine the activity of Ge doped by 11.0%, whereas the band gap, density of state, and optical properties were affected. Analysis of the band gap and optical properties of both of Mg $(BiO_2)_4$ and $Mg(Bi_{0.91}Ge_{0.083}O_2)_4$, the Ge doped shows the high conductivity than undoped.

Keywords: *Band Structure, $Mg(BiO_2)_4$, $Mg(Bi_{0.91}Ge_{0.083}O_2)_4$, DOS, PDOS, and Optical Properties.*

1. Introduction

The semiconductor technology, over the last 60 years, the continuous progress of compounds of class IV, II, VI, and III-V have been made [1]. The crystal field model has been very successful in the analysis of 4f configurations of rare-earth ions in solids, whose energy levels are reproduced through a Hamiltonian and involves both free-atom and crystal field operators [2, 3]. A satisfactory simulation of the experimental scheme of energy levels can be achieved if the number and quality of the operators are adequate. The use of semiconductors is increasing day by day. By combining multiple compounds, some semiconductor materials are tunable, for example, in the band gap [4, 5]. The result is a diagonal, quadrilateral, even curly compositions. Adjusting the band gap in the range of binary compounds involved in the tonary composition, however, in the case of the material combination of direct and indirect band gaps, there is a ratio where indirect band gap prevails, limiting the usability of the range for optoelectronics, Such loose LEDs are limited by 660 nm [6, 7]. The compositional polarizations of the compounds may also differ, and the explosion of the mesh against the substrate, based on the proportion of the mixture, defects to a degree depending on the imperfection. This affects the ratio of the achievable radiation or sequential reconnection and determines the illumination efficiency of the device. The quadrants and higher compositions coordinate the band gap and lane constant simultaneously, allowing for increased efficiency over a wide range of wavelengths [8]. For example the loose input is used for the LED. Transparent materials from light-generated

[1] Corresponding Authors

e-mail: kumarajoy.cu@gmail.com

wavelengths are useful, as it allows more efficient extraction of photons from the bulk of the material. That is, in such transparent materials, light production is not only limited to the surface. The effect of the photon extraction efficiency is dependent on the index of the reflection and the material [9-11].

Semiconductor materials can strongly absorb the UV visible light or energy as used photocatalyst [12-14]. There are different forms of absorption, but the most important is the absorption of the underlying band, that is, the band with or without the bandwidth equal to or better than the band electron absorption energy [15, 16], while transforming the transport band, leaving such valence band [17-20]. The electrons that jump from the conduction band can withstand a reduced response through the external circuit from the opposite pole. The hole has a strong oxidizing ability, which causes the oxidation reaction of the appropriate components of the solution. High purity silicon is an important semiconductor material. Monocrystalline silicon doped a small amount of Group IIIA components to form one-third silicon semiconductor [21]. When N-type and P-type semiconductors are simultaneously inserted a trace amount of N-form and P-type semiconductor group VA components, solar cells can be formed, the development of radiant kinetic energy in electricity is a promising element [22].

$Mg(BiO_2)_4$ minerals by virtue of their high heat resistance, lightweight weight, high elasticity constant, refraction crystal structure, antioxidative, anticorrosion, and antiwear properties [23-25]. As a result of these properties, the compound has intensive usage space and application potentials. $Mg(BiO_2)_4$ is also magnesium borates that have great potential in areas of electronic ceramic reinforcement, semiconductor material synthesis, and plastics or aluminum/magnesium matrix alloy production [26, 27]. In this case of applications in the electric device, $Mg(BiO_2)_4$ is the most acceptable material for electrochemistry as semiconductors. For using the $Mg(BiO_2)_4$, the aim of this study is to develop the theoretical concept using first principle study, and doping was done by Ge to increase their activity.

2. Computational Methods

The method of GGA with PBE was optimized for CASTEP code from material studio to calculate the band gap and density of state [28]. In this condition, the band gap and density of state were calculated using the cut off at 510, and k point at 2×2×4 with non-conserving pseudopotentials. Then the optical properties were similar way simulated for calculation of refractive index, reflectivity, absorption, conductivity, and loss function. In additionally, the geometric optimization was achieved and the convergence criterion for the force between atoms was 3×10^{-6} eV/˚A, the maximum displacement was 1×10^{-3}˚A, and the total energy and the maximal stress were 1×10^{-5} eV/atom and 5×10^{-2} GPa, respectively. In similar way, Ge was doped replacing Bi by 8.3% using building option and supercell option and finally all above properties using similar option was simulated.

3. Results and Discussion

3.1. Optimized Structure

The lattice parameters value are a = 3.394 Å b = 8.761.Å, c = 9.059 Å and angels between them as α= 69.566° β= 78.722° A°, γ= 78.373° A° for both of $Mg(BiO_2)_4$ and Mg $(Bi_{0.91}Ge_{0.083}O_2)_4$. The monoclinic $Mg(BiO_2)_4$ crystal and the space group is Hermanna Mauguin Cm, monoclinic crystal system, point group m, hall C$\bar{2}$y, density 6.70 g/cm^{3}shown in figure 1(a), and the Ge doped optimized structure in figure 1(b).

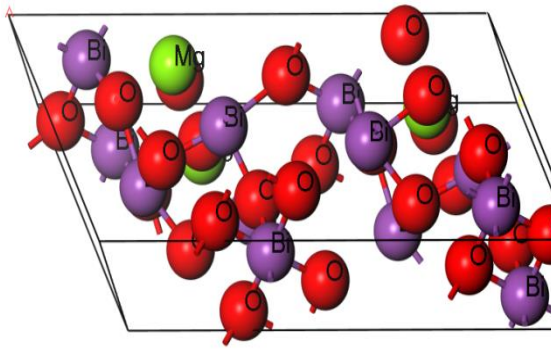

Fig. 1(a): Structure for $Mg(BiO2)_4$

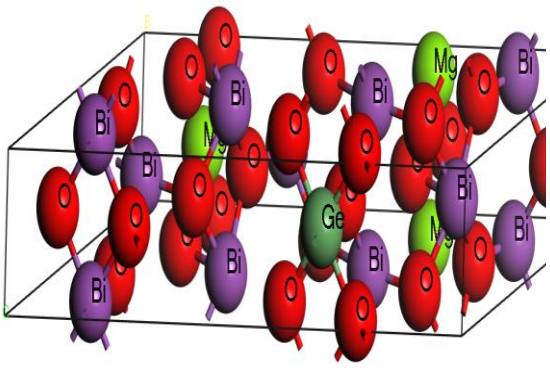

Fig. 1(b): Structure for $Mg(Bi_{0.91}Ge_{0.083}O_2)_4$

3.2. Electronic Structure

The electronic band structure of $Mg(BiO_2)_4$ and Mg $(Bi_{0.917}Ge_{0.083}O_2)_4$ was calculated in the Fermi energy level setting at zero. From the figure 2(a), it absolutely was found that the minimum of conduction bands (MCB) was obtained within the G symmetry point, whereas the maximum of valance bands (MVB) was connected additionally in G symmetry points. Because each MCB and MVB is at point G symmetry, it's known as a direct band gap, and it's calculated by 0.545 eV. Figure 2(a) represents the band structure of Ge doped while the MCB and MVB meet at G symmetry point indicating a direct band gap and recorded as 0.00 eV known as a superconductor. In general, a lower carrier effective mass corresponds to the next carrier mobility. On the opposite hand, after Ge doping in $Mg(BiO_2)_4$ shows a totally different band structure both of MCB and MVB.

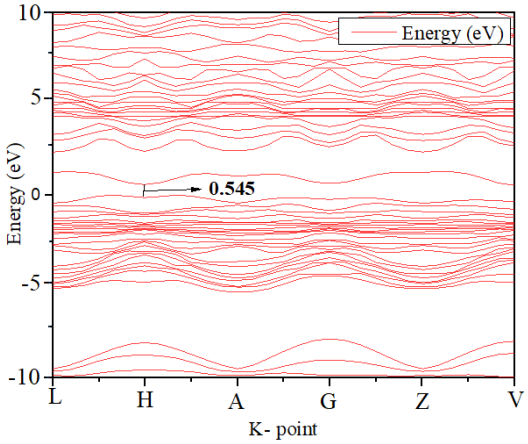

Fig. 2(a): Electronic structure for undoped

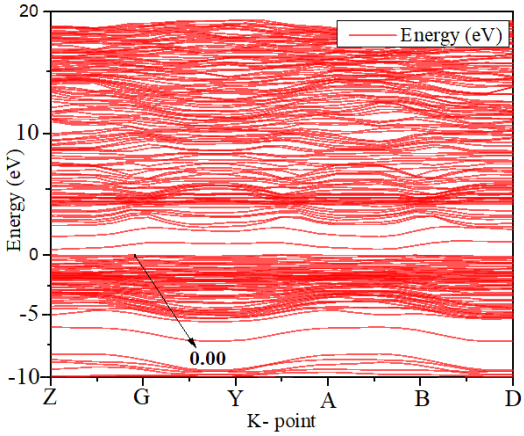

Fig. 2(b): Electronic structure for doped

3.3. The density of State and partial density of state

The density of the state indicates the character of electronic band structures and the splitting of an orbital. The density of states (DOS) of Mg, Bi, Ge, and O atoms of $Mg(BiO_2)_4$, and $Mg(Bi_{0.91}Ge_{0.083}O_2)_4$ crystals were calculated by PBE0 with GGA. From figure 3(a), it absolutely was found that the valence bands squarem measure primarily occupied by 3s for Mg, 6s 4f 5d 6p for Ge and 2s 2d for O atom. Meanwhile, on top of the Fermi level, the conductivity bands are composed of Mg in 3s, Bi in 6s 4f 6p 5d and O atom in 2s orbitals. As shown in figure 3, the bands just below the Fermi level and on top of the Fermi level, it's noted that the total density of state for doped Mg $(Bi_{0.91}Ge_{0.083}O_2)_4$ is higher than $Mg(BiO_2)_4$ and it's evaluated that the DOS for s, p, d and sum for doped is a lot of delocalized than undoped showing in figure 3(a), 3(b), 3(c), 3(d), 3(e), and 3(f).

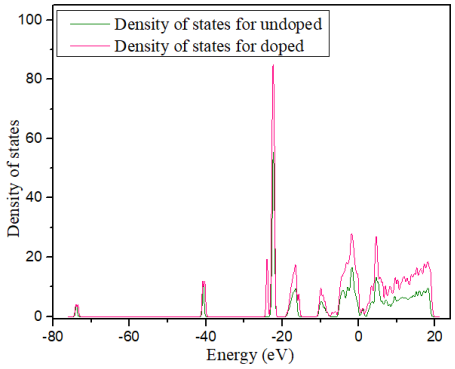

Fig. 3(a): comparison of total DOS for doped and undoped

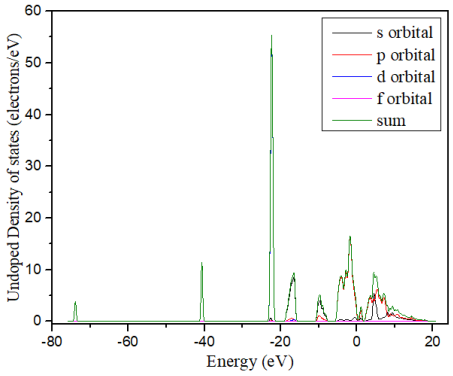

Fig. 3(b): PDOS for undoped

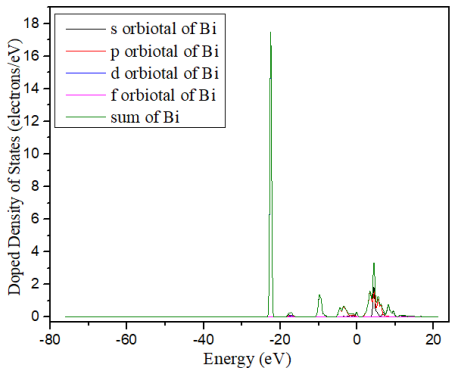

Fig. 3(c): PDOS for doped

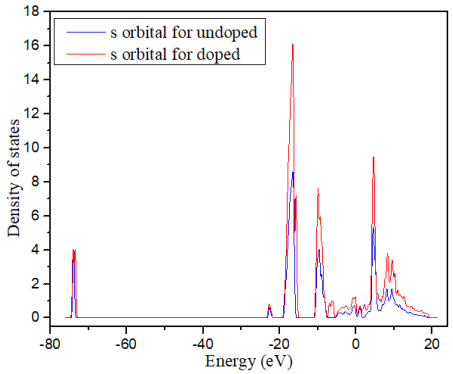

Fig. 3(d): comparison the DOS of s orbital for doped and undoped

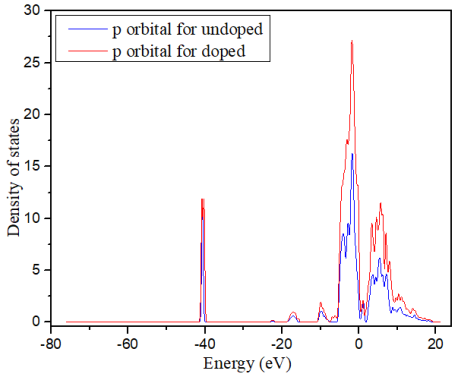

Fig. 3(e): Comparison the DOS of p orbital for doped and undoped

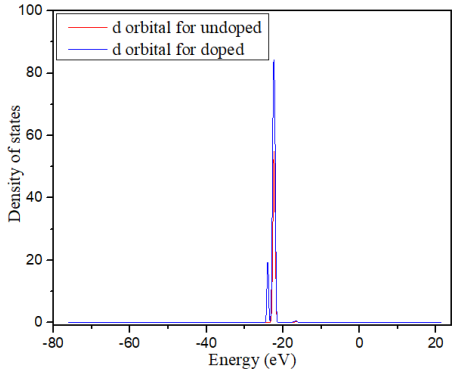

Fig. 3(f): Comparison the DOS of d orbital for doped and undoped

3.4. Optical Properties

3.4.1. Optical Reflectivity

As a section of many consecutive theoretical investigations of optical phenomenon, at first, we have a tendency to go through the quantification of optical reflectivity of a crystalline material as a result of it's a major role in the electronic transition from valance band to the conduction band of compounds. The number of the wavelength that's incident on the surface of the semiconductor materials that can be calculated from the reflectivity information, which is related to the observance of that material. It's reported in a number of previous investigations that the lower reflectivity indicates the upper UV or visible light absorption. In our investigation, we have a tendency to determine that the reflectivity of $Mg(BiO_2)_4$, and $Mg(Bi_{0.91}Ge_{0.083}O_2)_4$ commences from around 0.25 and 0.35 severally at initial frequency. From figure 4, there are small differenences between undoped and doped.

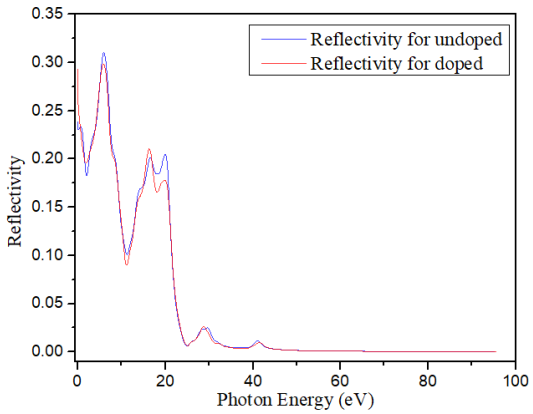

Fig. 4: Reflectivity

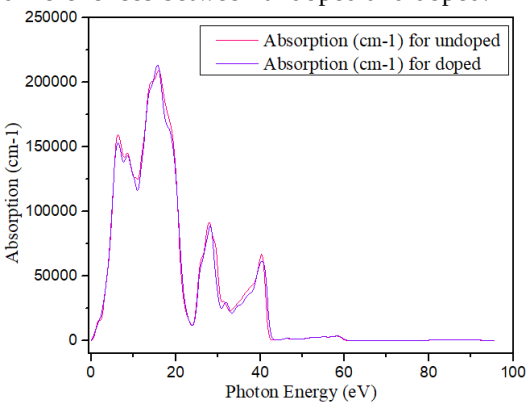

Fig. 5: Absorption

3.4.2. Absorption

The polycrystalline polarization technique is used to calculate the optical absorption of the $Mg(BiO_2)_4$, and $Mg(Bi_{0.91}Ge_{0.083}O_2)_4$ materials and also, the technique includes the electrical field vector as an isotropic average over all directions. During the simulation, a small smearing value of 0.5 eV was applied in order to attain additional distinguishable absorption peaks. The obtained absorption peaks, as represented in figure 5, are attributed to the image transition energies from the MVB to the MCB underneath visible light irradiation, which indicates that this material can absorb photons of visible range. Each of $Mg(BiO_2)_4$, and $Mg(Bi_{0.91}Ge_{0.083}O_2)_4$ shows the small deviation at the same point, but $Mg(Bi_{0.91}Ge_{0.083}O_2)_4$ is slightly higher than $Mg(BiO_2)_4$.

3.4.3. Refractive Index

The index of refraction of a material is an impactful parameter for mensuration of the photon absorbed throughout the method of chemical degradation from the solutions. Asa complements to index enhancing schemes involving lasing without inversion, ultra-refractive optics with photonic band materials have many applications, including laser accelerators and lenses of ultra-short focal length [29]. The Large value of the index of refraction is related to the larger, denser medium, which is according to a very previous investigation [30, 31]. Figure 6 displays the refraction index as a function of photon energy wherever the real part and, therefore, the imaginary part of a complex number for each of the undoped and doped are mentioned, showing an inverse pattern. At the initial point of photon energy in the refraction index is higher for the real part while the imaginary part of a complex number is nearly closed to zero. Subsequent overall, a decrease of each element encounters them to every other up to 23 eV by value from 3.3 to 0.1, and afterward, they follow a constant pattern overlapping to each other.

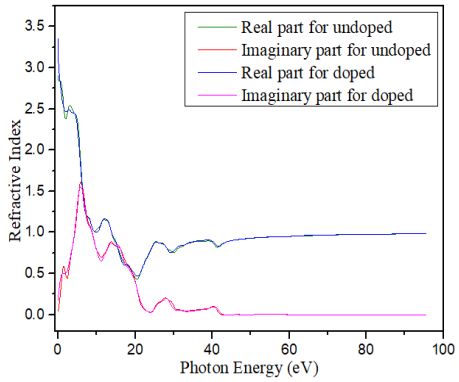

Fig. 6: Refractive Index

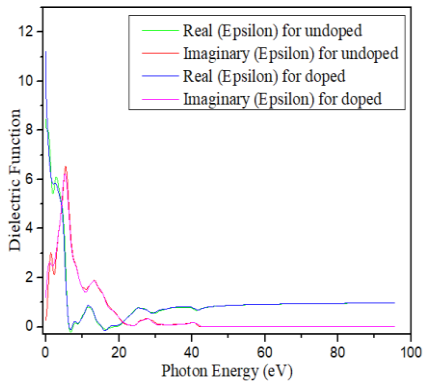

Fig. 7: Dielectric Function

3.4.4. Dielectric Function

The dielectric function is an incredibly necessary tool to analyze their optical properties that are expounded with sorption properties as the following equation for solid [32].

$$\varepsilon = \varepsilon_1(\omega) + i\varepsilon_2(\omega)$$

where $\varepsilon_1(\omega)$ and $\varepsilon_2(\omega)$ are denoted nonconductor constant (real part) and the dielectric loss factor (imaginary part) respectively. Nonconductor function includes a relationship with the space of materials that are physically equivalent to the permittivity or absolute permittivity. The real part of the dielectric function represents the energy storage capability in the electric field, and also the pure imaginary number represents the energy dissipation capability of the nonconductor materials. From the figure 7, the imaginary pure imaginary number is a smaller amount than the real part from 0 eV to 5 eV frequencies however from 6 eV to 16 eV, the imaginary part of a complex number pure imaginary number is larger than real part, showing same the real and imaginary part for the doped and undoped.

3.4.5. Conductivity

The physical phenomenon of the semiconductor on the basis of the energy band and orbital electrons is joined with the discrete parts of electrons in orbit. This can be conjointly made due to the presence of holes and free electrons within the crystal molecules. From figure 8, the physical phenomenon of doped is slightly larger than undoped within both cases.

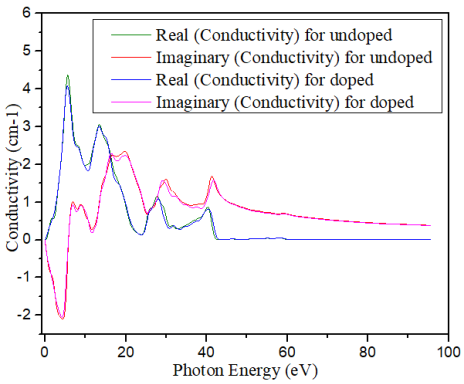

Fig. 8: Conductivity

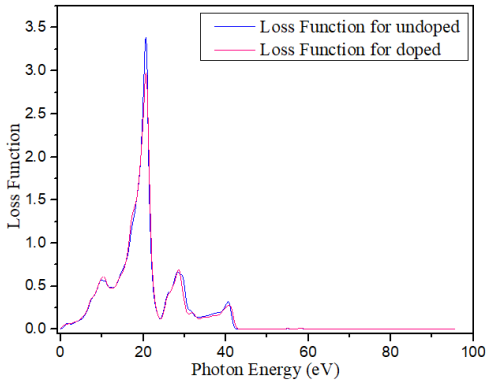

Fig. 9: Loss Function

3.4.6. Loss Function

There are two regions for the electronic energy loss function, such as high energy region or low energy region for optical properties. From figure 9, the loss function for doped is poor higher than undoped.

4. Conclusion

In this study, a comparative investigation was estimated between $Mg(BiO_2)_4$, and $Mg(Bi_{0.91}Ge_{0.083}O_2)_4$ using first principle method of generalized gradient approximation (GGA) on the Perdew–Burke–Ernzerhoff (PBE0). At first, the electronic structure of $Mg(BiO_2)_4$ is not well dispersive as $Mg(Bi_{0.91}Ge_{0.083}O_2)_4$ and the band gap of $Mg(BiO_2)_4$, and $Mg(Bi_{0.91}Ge_{0.083}O_2)_4$ are 0.545 and 0.00 respectively, indicating semiconductor and superconductor. Secondly Ge doping in $Mg(BiO_2)_4$ increases the DOS and optical properties. Mean that Ge doping increases the conductivity of examined crystals.

References

[1] G. D. H. Hutcheson, Jerry D, Technology and economics in the semiconductor industry, Scientific American. 274 (1996) 54-62.

[2] R. Boča, Magnetic parameters and magnetic functions in mononuclear complexes beyond the spin-Hamiltonian formalism. Magnetic Functions Beyond the Spin-Hamiltonian: Springer, 117 (2006) 1-264.

[3] M. G. Faucher, D. Caro, P. Derouet, J. Porcher, P, The anomalous crystal field splittings of 2H11/2 (Nd 3+, 4f3). Journal de Physique 50 (1989) 219-243.

[4] Y. X. Li, Yuanjiang. Wen, Shuangchun. Yong, Junhai. Fan, Dianyuan, Tunable terahertz-mirror and multi-channel terahertz-filter based on one-dimensional photonic crystals containing semiconductors. Journal of Applied Physics 110 (211) 073111.

[5] M. D. Regulacio and M.-Y. Han, Composition-tunable alloyed semiconductor nanocrystals. Accounts of chemical research 43 (2010) 621-630.

[6] J. L. Hudgins, G. S. Simin, E. Santi, M. A. Khan, An assessment of wide bandgap semiconductors for power devices, IEEE Transactions on Power Electronics, 18 (2003) 907-914.

[7] L. L. Gu, V. Srot, W. Sigle, C. Koch, P. V. Aken, F. Scholz, S. B. Thapa, C. Kirchner, M. Jetter, M. Rühle, Manfred Band-gap measurements of direct and indirect semiconductors using monochromated electrons. Physical Review B 75 (2007) 195214.

[8] K.-H. K. Park, Tae-Young; Han, Shin; Ko, Hyun-Seok; Lee, Suk-Ho; Song, Yong-Min; Kim, Jung-Hun; Lee, Jae-Wook, Light harvesting over a wide range of wavelength using natural dyes of gardenia and cochineal for dye-sensitized solar cells. Spectrochimica Acta Part A: Molecular and Biomolecular Spectroscopy 128(2014) 868-873, 2014.

[9] A. Badano and J. Kanicki, Monte Carlo analysis of the spectral photon emission and extraction efficiency of organic light-emitting devices. Journal of Applied Physics 90 (2001) 1827-1830.

[10] N. G. Narendran, Y; Freyssinier-Nova, JP; Zhu, Y, Extracting phosphor-scattered photons to improve white LED efficiency. physica status solidi (a) 202 (2005) R60-R62.

[11] S. J. Lee, Study of photon extraction efficiency in InGaN light-emitting diodes depending on chip structures and chip-mount schemes. Optical Engineering 45 (2006) 014601.

[12] M. M. Hasan, A. Ajoy, U. Chakma, Theoretical Investigation of Doping Effect of Fe for SnWO4 in Electronic Structure and Optical Properties: DFT Based First Principle Study. Advanced Journal of Chemistry-Section A 2020 (2020), no. In Press, 2020.

[13] M. J. Islam, A. Kumer, First-principles study of structural, electronic and optical properties of AgSbO3 and AgSb0.78 Se0.22O3 photocatalyst. SN Applied Sciences 2(2020) 251.

[14] B. C. A. Kamal, Kumer; Unesco, Chakma; Debashis, Howlader; Md Tawhidul, Islam;, A theoretical investigation for electronics structure of Mg(BiO2)2 semiconductor using first principle approach. International Journal of New Chemistry, vol. 2020, no. In Press, 2020.

[15] U. Chakma, A. Kumer, K. B. Chakma, M. T. Islam, D. Howlader, Electronics Structure and Optical Properties of Ag2BiO3,(Ag2) 0.88 Fe0. 12BiO3: A First Principle Approach, Advanced Journal of Chemistry. Section A: Theoretical, Engineering and Applied Chemistry 3 (2020) 542–550.

[16] U. Chakma, A. Kumer, K. B. Chakma, M. T. Islam, D. Howlader, Mohamed, Rasha M K, Electronics structure and optical properties of SrPbO3 and SrPb0. 94Fe0. 06O3: A first principle approach. Eurasian Chemical Communications 2(2020) 573-580.

[17] D. Wood and J. Tauc, Weak absorption tails in amorphous semiconductors. Physical Review B 5 (1972) 3144,.

[18] R. K. Waring Jr and W. Y. Hsu, Urbach rule behavior in strongly absorbing fine particle solids, Journal of Applied Physics 54(1983) 4093-4096.

[19] A. F. Henglein, Anton; Welter, Horst Reactions on colloidal semiconductor particles. Berichte der Bunsengesellschaft für physikalische Chemie 91 (1987) 441-446.

[20] E. Davis and N. Mott, Conduction in non-crystalline systems V. Conductivity, optical absorption and photoconductivity in amorphous semiconductors. Philosophical Magazine 22 (1970) 0903-0922.

[21] A. Addamiano, Preparation and Photoluminescence of Silicon Carbide Phosphors Doped with Group III a Elements and/or Nitrogen. Journal of The Electrochemical Society 113 (1966) 134-136.

[22] Y. T. Nakato, Akira; Tsubomura, Hiroshi, Efficient Photoelectrochemical Conversion of Solar Energy with N-Type Silicon Semiconductor Electrodes Surface-Doped with IIIA-Group Elements. Chemistry Letters 11 (1982) 1071-1074.

[23] A. D. Barros, R; Deschamp, J; Boutinaud, P; Chadeyron, Geneviève; Mahiou, R; Cavalli, E; Brik, MG, Optical properties and electronic band structure of BiMg2PO6, BiMg2VO6, BiMg2VO6: Pr3+ and BiMg2VO6: Eu3+. Optical Materials 36 (2014) 1724-1729.

[24] Y. W. Huang, Wei; Zhang, Qian; Cao, Jun-ji; Huang, Ru-jin; Ho, Wingkei; Lee, Shun Cheng, In situ fabrication of α-Bi 2 O 3/(BiO) 2 CO 3 nanoplate heterojunctions with tunable optical property and photocatalytic activity. Scientific reports 6 (2016) 23435.

[25] H. C. Punetha, M; Bhutia, S; Tripathi, Sonal; Prakash, Om, Antioxidative properties and mineral composition of defatted meal of oileferous Brassica germplasm. Journal of Biologically Active Products from Nature 5 (2015) 43-51.

[26] L. W. JI, Yu-min; SHI, Nan-lin, TEM Analysis of Interface in SiC Fibre Reinforced Aluminium Matrix Composite Prepared with Semi-solid Diffusing Method [J]. Journal of Materials Engineering 6 (2009) 46-50.

[27] H. L. QIAO, Qingtang; FU, Hanguang; LEI, Yongping, Microstructure and properties of in-situ synthesized ceramic phase reinforced Fe-based coating by laser cladding. Transactions of the China Welding Institution, (2015) 17.

[28] J. P. B. Perdew, Kieron; Ernzerhof, Matthias, Generalized gradient approximation made simple. Physical review letters 77 (1996) 3865.

[29] J. P. Dowling and C. M. Bowden, Anomalous index of refraction in photonic bandgap materials. Journal of Modern Optics 41 (1994) 345-351.

[30] F. P. P. Bolin, Luther E; Taylor, Roy C; Ference, Robert J, Refractive index of some mammalian tissues using a fiber optic cladding method. Applied optics 28 (1989) 2297-2303.

[31] X.-J. M. Wang, Thomas E; De Boer, Johannes F; Zhang, Yi; Pashley, David H; Nelson, J Stuart, Characterization of dentin and enamel by use of optical coherence tomography. Applied optics 38 (1999) 2092-2096.

[32] G. F. I. Bertsch, J, I; Rubio, Angel; Yabana, Kazuhiro;, Real-space, real-time method for the dielectric function, Physical Review B, vol. 62, no. 12, p. 7998, 2000.